ICSV13 - Vienna
The Thirteenth International Congress on Sound and Vibration
Vienna, Austria, July 2-6, 2006

COMPUTATIONAL AND EXPERIMENTAL INVESTIGATION ON 50-CENTIMETER VALVELESS PULSEJET

F. Zheng, R. L. Ordon, T. Geng, T.D. Scharton, A. V. Kuznetsov and W. L. Roberts

Department of Mechanical & Aerospace Engineering, North Carolina State University, Raleigh, NC 27606, USA
fzheng@ncsu.edu

Abstract
Due to its simplicity, the pulsejet may be an ideal micro propulsion system. In this paper, modern experimental and computational methods were used to study a 50-centimeter pulsejet to develop an understanding of how various inlets, exhaust sizes and free stream velocity effect the overall performance of the jet. Experimentally, pressure and temperature were measured at several axial locations under different fuel flow rates for different geometries. Simulations were made with the same geometries and fuel flow rate using CFX to develop further understanding of the factors that affect the performance of pulsejet.

Keywords: pulsejet; valveless;

INTRODUCTION

The pulsejet is an unsteady propulsion device that generates intermittent thrust. The reactants enter the tube when the pressure in the combustion chamber is lower than ambient pressure. Residual hot gases and heat transfer from the hot walls raise the reactant temperature above the auto ignition temperature, initiating ignition and combustion of the reactants. The ensuing heat release increases the pressure, and these hot gases then expand down the exhaust duct and exit at high velocity, generating thrust. The hot gases at the exit have expanded to nearly atmospheric pressure and their momentum causes an expansion wave to propagate back up the exhaust duct towards the combustion chamber. When the expansion wave reaches the chamber, the combustion chamber pressure becomes sub atmospheric and the cycle repeats itself.

The primary reason for the development of a valveless pulsejet is that in most designs, the use of reed valves limits the reliability and longevity of the engine, and renders the pulsejet difficult to scale down in size. In the valved pulsejet, the function of the intake valves is to prevent a reversal of the flow at the inlet – and therefore negative momentum transport – when the combustion chamber pressure exceeds the free-stream stagnation pressure. By proper utilization of wave processes in an inlet duct of adequate length, the amount of negative thrust can be minimized [1].

There are many designs of valveless pulsejets, which differ mainly by inlet and outlet geometry and arrangement. The pulsejet is based on the Humphrey thermodynamic cycle, where isochoric heat addition (combustion) follows an isentropic compression and isobaric heat rejection follows an isentropic expansion. Because there is no mechanical compression, the overall thermodynamic efficiency is low.

Because of there relatively low efficiency, the pulsejet was surpassed by the much more efficient turbojet and was put aside for decades following limited development in the 1940's and 1950's. In a turbojet, high efficiency is achieved through high compressor pressure rates. However, the compressor is a complex and expensive piece of turbo machine that consumes a large fraction of the chemical enthalpy. As the scale of turbo machinery is reduced, their efficiency decreases and therefore efficiency of a turbojet drops nonlinearly with size when it utilized in a micro propulsion system. Therefore, there may be applications where small scale, simplicity, cost and high thrust to weight ratio make the pulsejet attractive [2].

The purpose of this paper is to compare the performance of a valveless pulsejet with different geometries to find out how inlet and outlet geometry affects frequency, temperature, and thrust of a valveless pulsejet, leading to an optimization of the design and a set of scaling laws.

The pulsejet discussed in this paper is a modified version of the BMS (Bailey Machining Service) hobby-scale pulsejet where the original valved inlet is replaced with a straight pipe.

ACOUSTIC THEORY

Self-compression is one of the most important characteristics of pulsejets, so understanding this phenomenon is of considerable interest. Pressure oscillations in a pulsejet are amplified by an acoustic resonance. Traditionally, a pulsejet with valves is characterized as a tube closed at the valve end and open at the exhaust end, so the fundamental resonance occurs when the total length of the pulsejet is equal to one quarter of an acoustic wavelength. However, an acoustic investigation of the pulsejet with valves revealed that, because of the increased diameter of the combustion chamber, the frequency of a pulsejet with valves behaves as an acoustic one-sixth-wave oscillator [3]:

$$f_e = c_e/(6L_t)$$

Where f_e is the resonate frequency associated with the exhaust pipe, c_e is the average speed of sound in the exhaust tube, and L_t is the total length of the pulsejet, excluding the inlet.

The inlet length is much shorter than the than the exhaust, only a few diameters long and thus much shorter than the sound wavelength. Therefore, the combination of this short inlet and combustion chamber is modeled as a Helmholtz resonator. The frequency of a Helmholtz resonator may be calculated as:

$$f_i = [c_i/(2\pi)][S/(VL_i)]^{0.5}$$

Where f_i is the resonate frequency associated with the inlet, c_i is the average speed of sound in the inlet and combustion chamber, S is the cross section area of the inlet, V is the volume of the combustion chamber, and L_i is the length of the inlet.

The sound speeds in these two equations are proportional to the square root of the space-time average temperatures.

EXPERIMENTAL SETUP

As shown in Fig. 1, the pulsejet is composed of 3 parts: valveless head, body, and extension. Ports 1 through 5 were added to allow temperature and pressure measurement. Four valveless heads were made at different diameters (1.3, 1.6, 2.2 and 2.5 cm) and different length (2.54, 5.08 and 7.62 cm) to determine geometry effects on performance. Aluminium had been chosen at first but was changed to steel because the inlets made of aluminium were deformed due to high temperature. A fuel injector was added to the pulsejet. It was made of 3 mm stainless steel tube with holes drilled through on it and was put in the combustion chamber at the axial position as port 1 but 90˚ to the position of port 1. An extension also added to the pulsejet to evaluate the contribution of a tailpipe length to the valveless pulsejet.

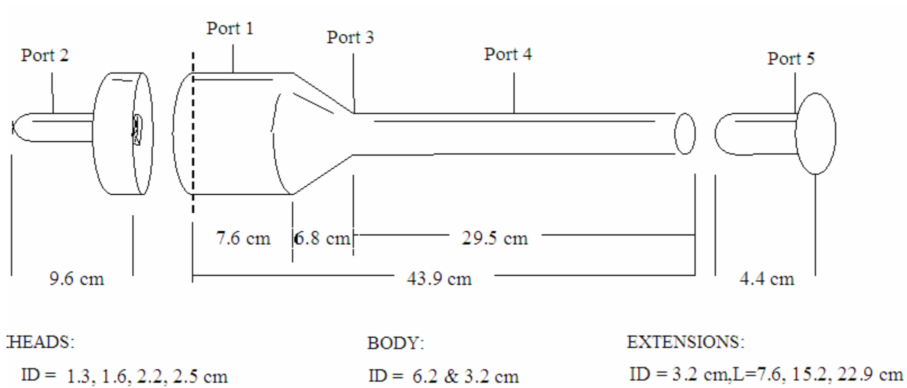

Figure 1: Dimensions of Experimental Jet

Propane was used as fuel to run the pulsejet. It is to compare test results with simulations, and propane combustion is relative simple to simulate. Fuel was fed into the system via a 0-30 SLPM (air) Hastings Flow Meter and Hastings Instruments Model 40 flow meter.

Type B thermocouples (platinum and platinum / rhodium) were used to measure average temperature. The voltage was measured with a Pentium 4 computer via a data acquisition card with a maximum input of 4 Hz per channel. Three thermocouples were used simultaneously to measure temperature at ports 1, 3 and 5 along the jet axis.

Both time-average and instantaneous pressures were measured at various axial locations in the jets. To measure the average pressure, a mercury manometer was used and placed on the side ports of the jet via an extension hose. For instantaneous pressure, a Kulite XTE-190-5G pressure transducer connected to a 12-V battery was utilized. A battery was required due to the AC to DC inverter making too much noise in the data. This pressure transducer was connected to an HP54503A Oscilloscope. Data was then transferred to a computer via GPIB to allow spreadsheet analysis of the data. More information about experimental setup is available in reference [4].

NUMERICAL MODEL

The commercially available CFX 5.7 package was used to model the combustion and flow inside and outside of the pulsejet. Because the pulsejet is symmetric about the axis, the geometry was made two-dimensional to save computational time. Total number of nodes in this model is about 18,000. The computations are performed on the NC State IBM Blade center utilizing a single 3.0 GHz Inter Xeon processor. Typical computational time for one cycle of the pulsejet is about 18 CPU hours.

k-ε model based on the Reynolds Averaged Navier-Stokes (RANS) equations was used because it offers a good compromise in terms of accuracy and robustness [5]. The Eddy Dissipation model was chosen as combustion model. A propane-air 5 step reaction mechanism was used to simulate the combustion process.

The computational domain included the flow field surrounding the pulsejet, not just interior flow. Because the boundaries are set so far from the pulsejet, effects from pulsejet operation are negligible and the boundary condition is set at 300 K temperature and 1 bar pressure.

There is significant heat flux between the pulsejet walls and fluid inside the pulsejet. However, the frequency is high enough and the thermal inertia large enough such that the wall temperatures are constant. Thus, a steady state simulation was performed based on measured average gas temperature, providing a wall temperature distribution. This was further simplified to what is shown in Fig. 2, a constant temp of 1000 K along the combustion chamber and then an exponential decay towards both the inlet and exit planes at 400 K.

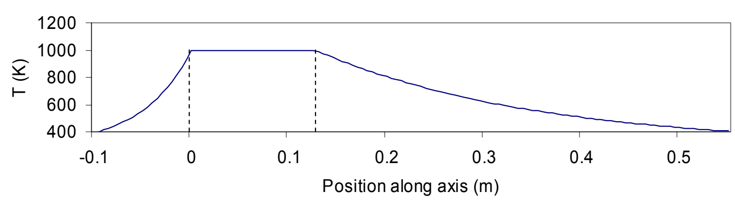

Figure 2: initial temperature distribution along the pulsejet

Pulsejets running at different forward flight speeds are also modelled by mimicking a wind tunnel with different incoming flow velocities. This is achieved by changing the boundary condition at the inlet of the enclosure flow field.

DATA ANALYSIS

The instantaneous pressure at port 3 is shown in Fig. 3 for a pulsejet with a 1.6 cm inlet diameter and 0.5 m tailpipe length. The high frequency oscillation in the experimental data is white noise from the power supply of the pressure transducer. From this comparison between experimental and computational result, two effects can be observed. First, the amplitude of pressure variation is almost the same in experimental and computational data; second, frequency observed in computational data is a little larger than that in experimental data.

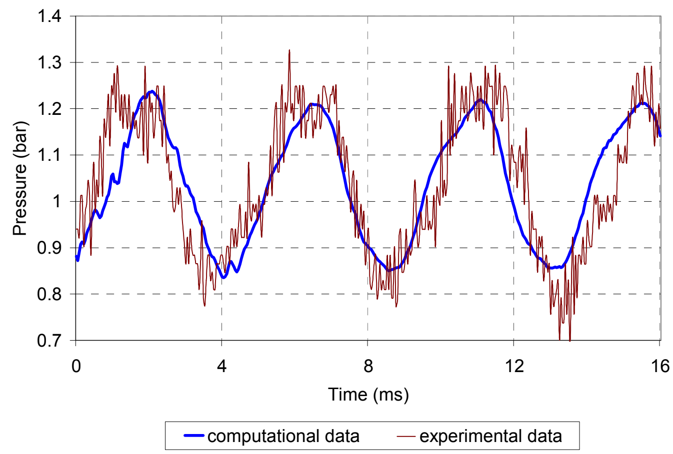

Figure 3: Chamber pressure for 1.6 cm inlet diameter and 0.5 m tailpipe length

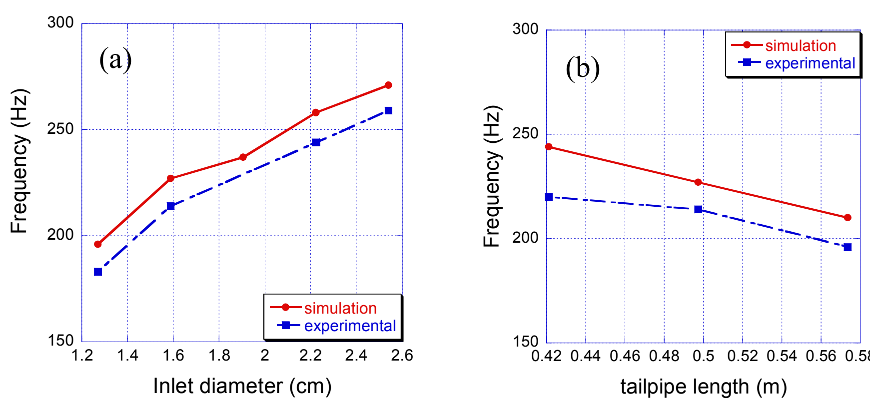

Figure 4: Frequency comparison between computational and experimental results.
a) Frequency Vs. inlet diameter for 0.5 m tailpipe pulsejet;
b) Frequency Vs. tailpipe length for 1.6 cm inlet diameter.

Because of the noise, it is difficult to identify the local minima & maxima of pressure for the experiment. However, frequency is obtained relatively accurately by taking the average value for several cycles. This frequency is generated by both the acoustic waves travelling in the tube, and the gases flowing into and out of the tube due to the large pressure differences. So this frequency contains information about all the properties relative to combustion, flow and heat transfer. As shown in Fig. 4, both experimental and computational results show a frequency increase with the increase of inlet diameter and decrease with the increase of tailpipe length.

As seen, the frequencies obtained from simulation results are 5-10% higher than those from experimental results. These disagreements could be explained by considering the temperature difference between experiments and simulates. As shown in table 1 (although experimental temperature for 2.2 cm inlet diameter pulsejet were not acquired due to thermometer malfunction), it is found that the average temperature from the simulations at port 3 are much higher than measured. This was caused by the fuel source point distribution; in the simulation point, we use a 4 degree wedge for two-dimensional computation, and have 90 point fuel sources for the whole pulsejet. However, in the experiments, there are only 8 source points in the fuel injector. Because the reaction is controlled by fuel-oxygen mixing in this case, it leads to a significantly quicker combustion in simulation than in experimental. That is the result of the compromise between precision and simulation time expense.

Table 1: chamber temperature from simulation and experimental

Inlet diameter (cm)	1.3	1.6	2.2	2.5
Simulation temperature (K)	1711	2000	1826	1807
Experimental temperature (K)	1593	1423	N/A	1343

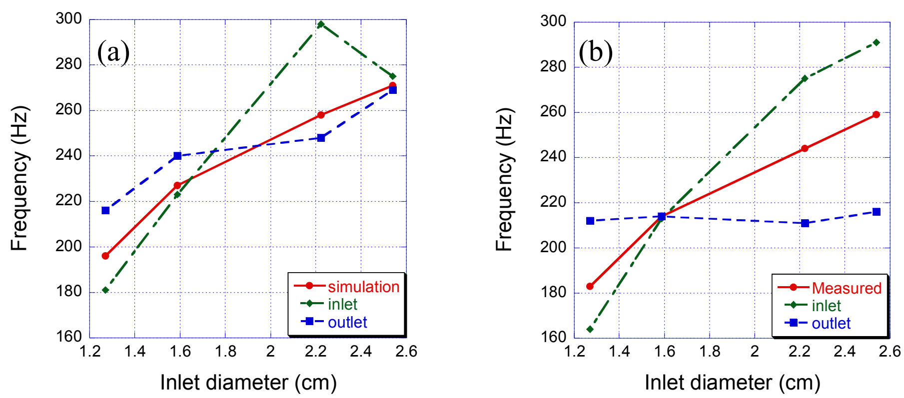

Figure 5: calculated inlet and outlet frequency compared with pulsejet running frequency for 0.5 m tail pipe. a) computational data; b) experimental data.

Fig. 5 compares the frequency calculated by Helmholtz resonator model (inlet) and 1/6 wave tube theory (outlet) with experimental and simulation data. From the figures, it is clear that the frequency from both the simulation and the experiment fit the average of the frequency calculated by the two analytical acoustic models very well.

These calculated frequencies are closely related with inlet and outlet temperature. Average temperature at inlet and outlet provide some information about the relative amount of time during each cycle that air is flowing into the pulsejet, from both ends, and products flowing out, also from both ends. As shown in Fig. 6, with a small inlet diameter, the average temperature of fluid moving through, the inlet is higher than the exhaust. As the inlet diameter increases, the inlet average temperature decreases while the exhaust average temperature increases. This is counter-intuitive, as one would expect a small diameter inlet to force more hot products out the exhaust. The computation and experiments agree quite well, but this phenomenon is still under investigation.

The numerical model is thus validated by comparing experimental and computational results for both temperature and pressure at various locations, as well as operating frequency.

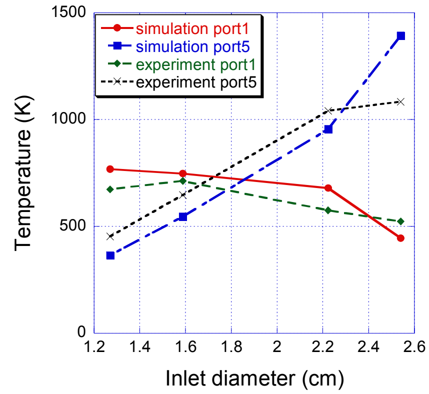

Figure 6: inlet and exit temperature vs. inlet diameter for 0.5 m tailpipe pulsejet

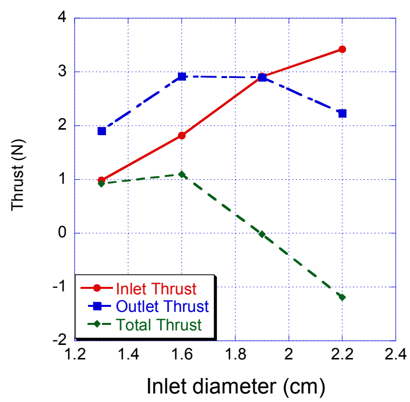

Figure 7: Thrust vs. inlet diameter

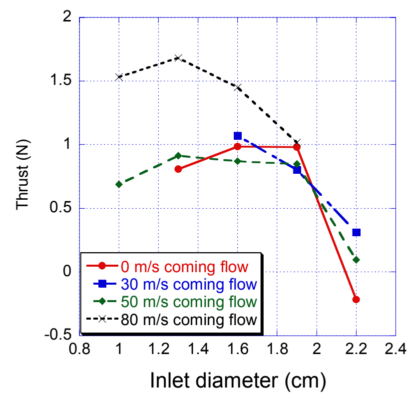

Figure 8: Thrust vs. inlet diameter for different coming flow speed

Thrust was not measured experimentally, but was calculated based on momentum flux through the inlet and exhaust. Fig. 7 shows calculated thrust for 0.5 m tail pipe length pulsejet with 0.47 g/s fuel flow rate as a function of inlet diameter. Total thrust is calculated by deducting the inlet thrust from the exhaust thrust. From this, it is clear that due to the increasing thrust at the inlet, the total thrust for the pulsejet reach its peak value at an inlet diameter of 1.6 cm, yielding an inlet to exhaust area ratio of 0.25.

Simulations were also performed for the cases with a free stream velocity. Results were obtained for 0.42 m tailpipe pulsejet with 1.0-2.2 cm inlet diameter and 0.47g/s fuel flow rate at 0 (static), 30, 50 and 80 m/s free stream velocity; the results are shown in Fig. 8. As the flow and flight speed increases, the inlet diameter at maximum thrust decreases.

From the simulations, it was found that the fuel flow rate and inlet diameter were coupled to the forward flight speed. For example, at 1.0 cm, the pulsejet would not work at 0.47 g/s at static, but would run at forward speed of 80 m/s. Conversely, at 2.2 cm, the pulsejet would run at static but not at 80 m/s unless the fuel flow rate was increased. In other words, fuel flow rate must be increased or inlet diameter must be decreased to keep the pulsejet running while forward flight speed increases.

CONCLUSIONS

From data analysis above, the following conclusions are obtained:

1. The operating frequency of the pulsejet depends on the average sound speed (dictated by temperature) and the geometry of both the inlet and outlet. The average of the frequencies calculated with the one-sixth wavelength equation for the exhaust pipe and the Helmholtz equation for the inlet tube fairly accurately predicts the operating frequency of the pulsejets in both the simulations and the experiments. The operating frequency increases when the inlet diameter is increased and when the exhaust pipe length is decreased.
2. The two-dimensional model simulates the experiment reasonably well. Different fuel supply modes result in the chamber temperature and frequency in the simulation being higher than in the experiment.
3. When inlet diameter is increased, average inlet temperature is decreased and average exit temperature increased, and there is more net mass flow travelling through the pulsejet.
4. As the forward speed increases, peak thrust occurs at smaller inlet diameters. To maintain operating, the inlet diameter must decrease and/or fuel flow rate increase as forward speed increases.

REFERENCES

[1] Foa, J. V., Elements of Flight Propulsion, John Wiley & Sons, New York, 1960.

[2] Ogorelec, B., “Valveless Pulsejet Engines,” URL: http://www.pulse-jets.com/valveless/.

[3] T. Travis, T. Scharton, A. Kuznetsov, W. Roberts, “The Principles of Operation of a Pulsejet with Valves,” 13th International Congress on Sound and Vibration, 2006.

[4] Ordon, R. L., “Experimental Investigation of 50cm Class Valveless Pulsejet Engines,’’ Master Dissertation, Mechanical and Aerospace Engineering Dept., North Carolina State Univ., Raleigh, NC, 2006.

[5] “Turbulence Models,” CFX-5 Solver Modelling, 103-118, (2004).